Determining of Flow Non-equilibrium Regions using the Kolmogorov-Smirnov Criterion

E. V. Titov, R. Kumar and D. A. Levin

Pennsylvania State University, University Park, PA 16802

Abstract. Studies of equilibrium breakdown were done for two flow problems representative of typical conditions for vehicles reentering the Earth atmosphere. The first studied problem was a 81 km Crew Exploration Vehicle (CEV) re-entry flow, with additional considerations for local flow features along the stagnation line. The second problem was a classical Couette flow, a volume of gas confined between two fast moving parallel plates of indefinite length and width. Both of the problems were solved by the DSMC technique with the particle velocity data collected to compute the distribution function at the areas of interest. In the case of stagnation line flow, a strong shock wave, formed in front of the vehicle at an altitude of 81 km was studied, and in the case of Couette flow, a high velocity boundary layer was examined in details at different Knudsen numbers. For both of the cases the Kolmogorov-Smirnov (K-S) test was applied to determine the degree of local flow non-equilibrium with following considerations regarding the applicability of coupled statistical BGK and DSMC techniques in the semi-rarefied flow regimes where the use of the baseline DSMC is limited due to the computational cost.

Keywords: DSMC, BGK, Flow Equilibrium, reentry
PACS: 05.20.Jj

THE MODELING PROCEDURE

The technique used in this research was the majorant frequency DSMC scheme [1]. The baseline DSMC modeling was applied using the SMILE [1] code. In the case of the Couette flow, a 2D computational domain was used to model an essentially 1D problem in anticipation of the complex 2D and 3D boundary layer flow studies requiring the local flow equilibrium analysis and in the case of the shock wave, a Crew exploration vehicle (CEV) shaped body subjected to a flow at 81 km was chosen as a test case. The flow parameters for both of the problems and numerical parameters of the DSMC scheme are presented in table at the end of the paper.

To study the degree of non-equilibrium in the flow we used the Kolmogrov-Smirnov (K-S) criterion. The K-S criterion provides a quantitative measure of difference between the computed (based on the sampled particle velocities) cumulative distribution function and a theoretical cumulative distribution function such as Maxwellian. In these studies we computed the distribution function by sampling the flow velocities at a number of locations, and the Maxwellian distribution function was defined by the local translational temperature of the modeled flow. The value of K-S criterion was computed as follows: The particle velocities were sampled during an extended period of computational time after the solution steady state was reached. The sampled velocities were arranged in an increasing order and then the maximum difference between the computed cumulative distribution function and locally defined Maxwellian one was obtained as follows:

$$D_n = max(F(x_i) - A(x_i)) \tag{1}$$

where $F(x_i)$ and $A(x_i)$ are the observed (computed) and assumed (Maxwellian in our cases) CDFs at the ith observation of the ordered samples. In the presented study we slightly modified the K-S criterion. Instead of arranging data in an increasing order, we place it into different velocity bins and then for each of the bins, we compute the CDFs using the data arranged in these velocity bins. The maximum difference is then found as follows:

$$D_n = max(F(i) - A(i)) \tag{2}$$

where $F(i)$ and $A(i)$ are the observed and assumed CDFs at the ith velocity interval.

RESULTS AND DISCUSSION

Couette flow

The first solved problem was a planar Couette flow. The gas flow took place without any pressure gradient between the plates that were parallel and moving with a constant velocity of ± 500. The height of the channel was 0.5 m, and the Knudsen number varied from 0.01 to 0.5 for different sub-cases. The plates were maintained at the same and constant temperature of T_p=273 K, which was equal to the free stream temperature.

The computational domain for the Couette flow problem is presented in Fig. 1, where the flow streamlines and velocity contour plots are also shown. As can be seen in the figure the equal velocity contours are parallel to the walls and the flow pattern is correct as illustrated by the streamlines, which indicates that the 1D problem is accurately solved by a 2D code.

The computed distribution function was based on one million samples of particle velocities collected after the solution steady state was reached. The chosen critical value of the K-S criterion was 0.005 [2] which meant that if the difference between the computed and local Maxwellian cumulative distribution functions was smaller than the critical value, the flow was considered to be in the state of equilibrium.

Portions A and B of Figure 2 show respectively the non-dimensional velocity and temperature profiles for three Couette flow sub-cases with Knudsen numbers respectively 0.01,0.1 and 0.5. Expectedly the temperature maximum is observed at the middle station across the plates, for all three cases, where the flow velocity is zero. Portion C of Fig. 2 shows the difference between the local Maxwellian distribution function and the computed one at the wall of the channel for Knudsen 0.5 case, and portion D of the figure shows the K-S parameter profiles for all three cases along with the equilibrium limit of the parameter shown as a dashed line.

It can be seen in the figure that for the first case of Kn=0.01, the K-S value remains within the equilibrium limit, hence showing that the flow is essentially continuum at this Knudsen number. The K-S parameter deviates slightly from the limit for the second case of Kn=0.1 showing a non-equilibrium behavior of the flow. For the third case of Kn=0.5, the K-S parameter deviates significantly from the equilibrium limit demonstrating a significant degree of non-equilibrium in the flow and therefore suggesting that a strict kinetic consideration of the flow is necessary.

Stagnation line shock wave

The computational domain for the shoch layer CEV case is presented in Fig. 3, where mole fraction contour plots of molecular and atomic nitrogen and linear plots of species mole fractions are also presented. One chemical reaction: the molecular nitrogen dissociation was modeled. As can be seen in the figure, the overall flow pattern is correct and the molecular nitrogen dissociation in the shock layer is modeled as expected.

The velocity distribution functions sampled at several locations across the shock layer for molecular and atomic nitrogen are presented in Figs. 4 and 5 respectively in comparison with locally defined Maxwellian velocity distribution functions. As the flow progresses through the shock layer the molecular nitrogen velocity distribution function, initially Maxwellian, deviates strongly from the equilibrium and then becomes again close to Maxwellian distribution function in the stagnation area in front of the body. The atomic nitrogen distribution function is harder do sample at the upstream edge of the shock layer since very few molecules of nitrogen initially dissociate to produce atomic nitrogen. To visualize the amount of atomic nitrogen, its mole fraction is presented in the rightmost portion of Fig.3 in comparison with molecular nitrogen mole fraction across the shock layer. The atomic nitrogen distribution function sampled at several locations across the shock layer, presented in 5 deviates from the Maxwellian one inside the shock layer, however becomes close to Maxwellian after the shock faster compared to molecular nitrogen distribution function. Such an observation can be done by comparing velocity distribution functions sampled at the same locations and presented in Figs.4 and 5 for molecular and atomic nitrogen respectively.

An interesting feature of the flow is presented in the third from the left portion of Fig. 4, where molecular nitrogen velocity distribution functions obtained at a location behind the shock is presented. The feature becomes apparent when the figure is compared with atomic nitrogen distribution function sampled at the same location in the flow and presented in the third from the left portion of Fig. 5. Both of the functions are compared with the Maxwellian distribution function defined by the local translational temperature. As can be seen in the figures there is a difference between the shapes of the molecular and atomic velocity distribution functions. The molecular nitrogen distribution function shows a bimodal profile and a stronger deviation from equilibrium while the atomic nitrogen distribution

function is closer to the Maxwellian one and does not show any bimodal behavior. The bimodal velocity distribution in the case of molecular nitrogen is due to the molecules reflected from the wall and molecules coming from the shock layer forming two distinct populations of particles. In the case of atomic nitrogen, on contrary, there is no second population in the velocity space since nitrogen atoms coming from the wall relax to the local state of equilibrium faster compared with the molecular nitrogen. Atomic nitrogen does not have internal degrees of freedom and therefore requires less collisions to reach the local state of equilibrium.

Results including both species are presented in Figs. 6 and 7. Figure 6 presents the distribution function obtained at several locations along the flow stagnation line. Portion (A) of the figure presents the distribution function at a location x=-0.623 m (before the shock) in comparison with the equilibrium distribution function defined by the local translational temperature. As can be seen in the figure the profile of the computed velocity distribution function is close to that of the local equilibrium velocity distribution function. This observation (which is also confirmed with the K-S studies) indicates the state of equilibrium in the undisturbed flow in front of the shock. However, as the flow enters the shock layer the profiles of the computed distribution function and the locally defined equilibrium one deviate from each other as can be seen in portions (B) and (C) of Fig. 6 where velocity distribution functions taken at locations x=-0.421 and x=-0.403 are presented. The strongest difference is observed at a location of x=-0.403 (portion (C) of Fig. 6, which corresponds to the middle of the shock layer. As the flow exits the shock layer region and stagnates in front of the body, the computed distribution function becomes close to the equilibrium one once again as presented in portion (D) of Fig. 6.

The results of the K-S studies for the CEV case are presented in Fig. 7 where the K-S criterion values are shown along the stagnation line. Also shown in the figure are the translational, rotational and vibrational temperatures to articulate the effect of non-equilibrium in the flow. As can be seen in the figure the degree of difference between the temperature profiles is expectedly large in this strong gradient flow, what is less obvious however is the behavior of the K-S criterion profile. The K-S value indeed increases significantly in the shock layer constituting a strong deviation from equilibrium, however, such a deviation occurs even before the flow reaches the shock layer (observe the difference in the behavior of the K-S criterion and the temperature profiles in Fig. 7). This difference is due to the fastest molecules (coming from the shock layer) ability to penetrate the flow upstream and this is why the effect of the presence of the shock can be observed at some distance upstream to the shock. This also means that in a coupled BGK/DSMC scheme the regions of application of a more accurate DSMC scheme may not be exactly identified based on the macro-parameters and their gradients alone, and more comprehensive kinetic approaches, based on the distribution function and criteria such as K-S criterion are necessary.

CONCLUSION

In this work we tested the K-S criterion as a tool to determine the non-equilibrium portions in semi-rarefied flows. We studied two different problems: a strong shock wave problem and a weak gradient Couette flow. We found it possible to quantify the degree of non-equilibrium in both of the studied flow cases indicating that the K-S criterion can be used to locate the areas of non-equilibrium. Although the baseline technique used in this work was the DSMC technique, the data necessary to compute the values of the criterion can be obtained instead from any statistical solver capable of accounting for the non-equilibrium properties in the flow. One of such techniques can be the statistical BGK method which is less computationally demanding than the baseline DSMC. Based on the results of the statistical BGK solution the areas of local non-equilibrium can be found and solved with a more accurate, but also more expensive, DSMC method. This will provide a foundation for a coupled BGK-DSMC (particle-particle) technique of an increased efficiency and high accuracy in the semi-rarefied flow configurations. Development of such a technique is the ultimate goal of this research.

ACKNOWLEDGMENTS

The authors would like to acknowledge support from NASA Grant NNX08AD84G from NASA/Johnson Space Flight Center.

REFERENCES

1. M. Ivanov, and S. Gimelshein, "Current Status and Prospects of the DSMC Modeling of Near-Continuum Flows of Non-reacting and Reacting Gases," in *Proceedings of the Rarefied Gas Dynamics 23rd Int. Symp., AIP Conference*, 2003, vol. 663, pp. 339–348.
2. A. Haldar, *Probability, Reliability and Statistical Methods in Engineering Design*, John Wiley and Sons, Inc., 2000.

Height, km	81	
Velocity, m/sec	7600.0	
Temperature, K	189.0	
Number Density, $1/m^{-3}$	$1.98 \times 10^{+23}$	$2.9 \times 10^{+19}$
N_2 Mole Fraction	100%	78.685%

CEV 81 km. (Atmosphere model: MSIS-E-90).

	Couette flow	DSMC, 81 km CEV case
Number of cells	164,860	2,124,130
Number of particles	33,821,840	20,900,300
Timestep, sec	1.0×10^{-8}	1.0×10^{-8}
Number of processors	16	32

DSMC scheme. Numerical parameters.

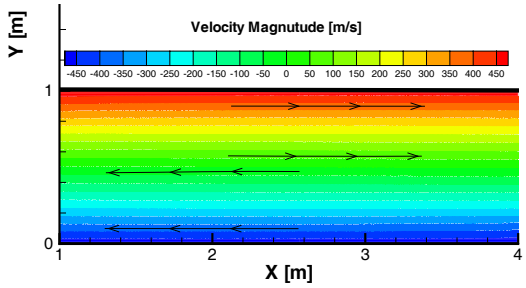

FIGURE 1. Kn = 0.01 Couette flow computational domain and flow streamlines.

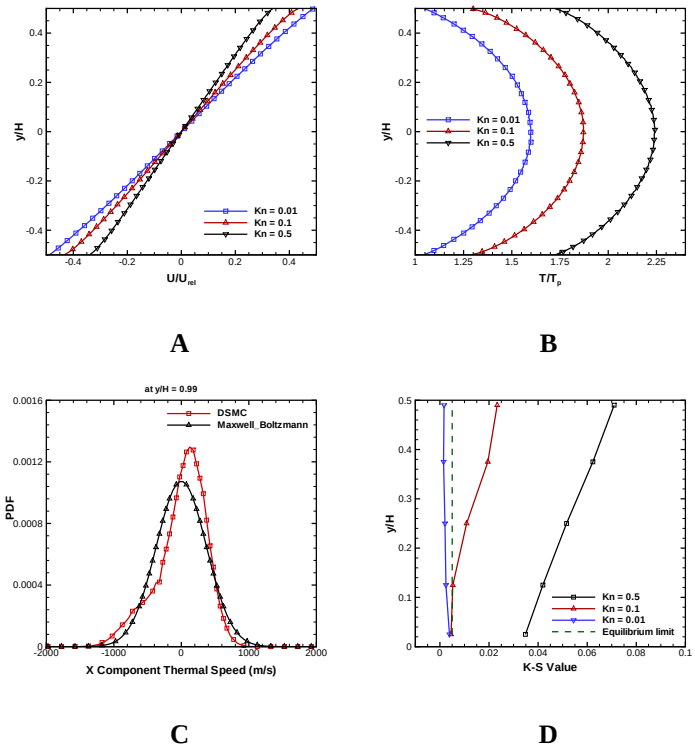

FIGURE 2. Couette flow 0.01,0.1, and 0.5 cases. A: Velocity profile, B: Temperature profile, C: distribution functions at the wall at Kn=0.5, D: K-S values.

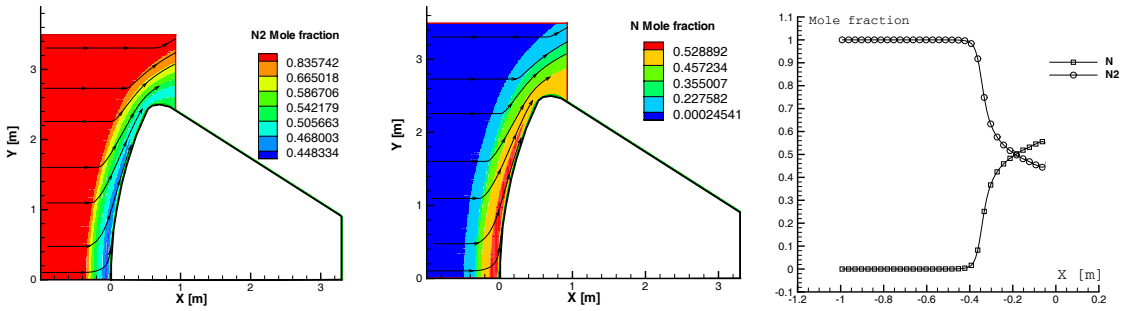

FIGURE 3. 81 km CEV case mole fractions, Left: N_2, Center: N, Right: N_2 and N

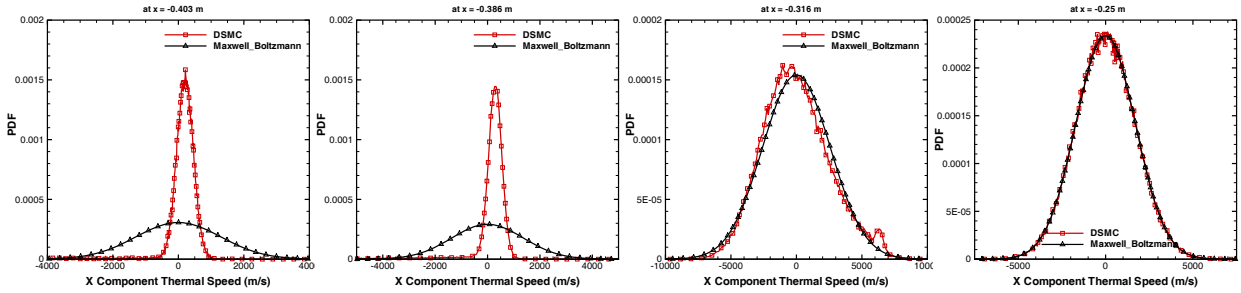

FIGURE 4. N_2, velocity distribution function samples across the shock layer.

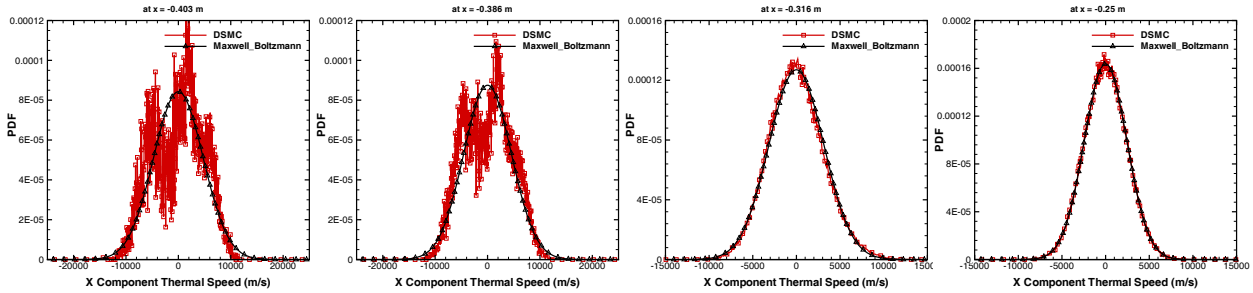

FIGURE 5. *N* velocity distribution function samples across the shock layer.

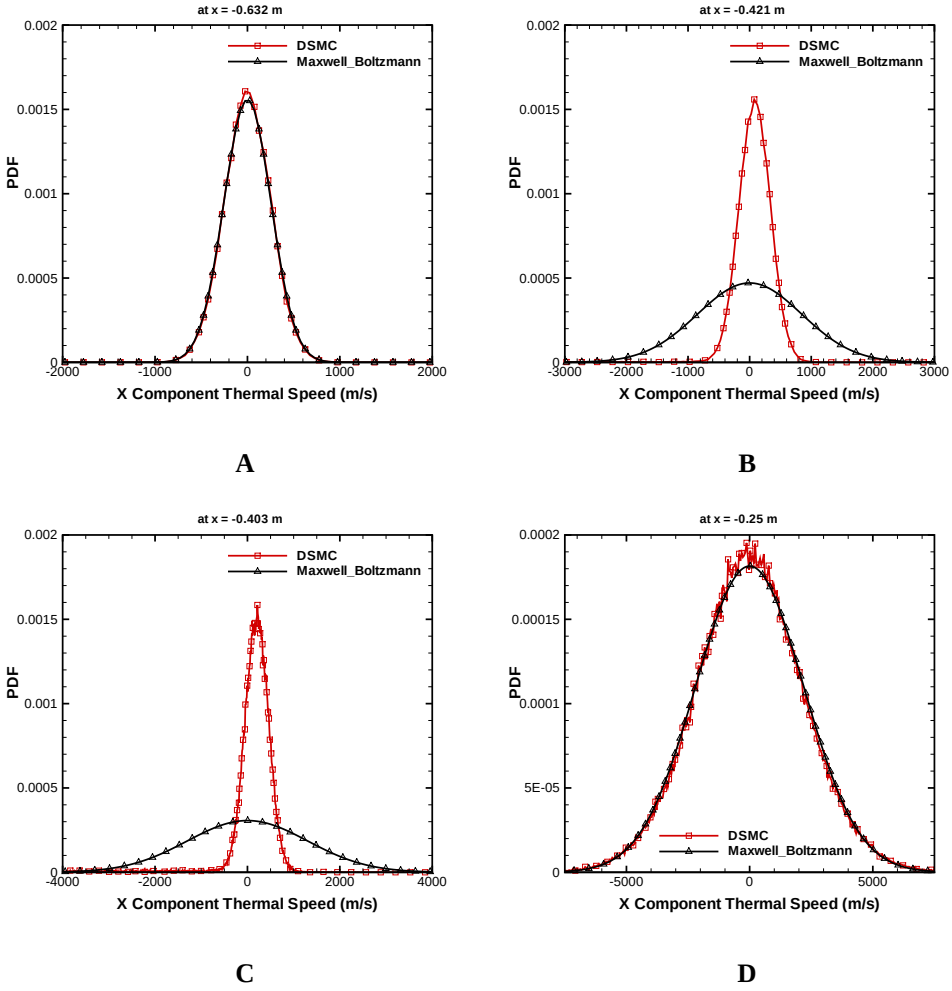

FIGURE 6. 81 km CEV shock wave case. Velocity distribution function. A: before the shock, B: inside the shock, C: inside the shock, D: after the shock.

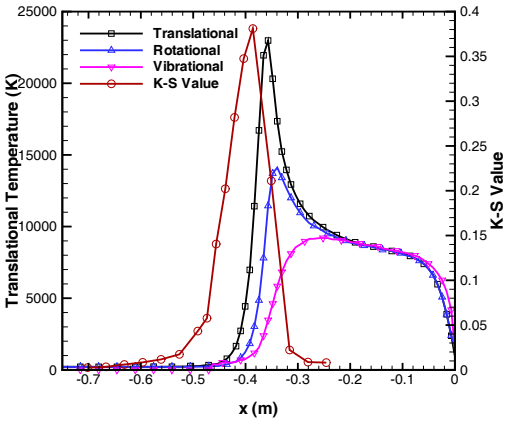

FIGURE 7. Kolmogorov Smirnov criteria value and translational, rotational and vibrational temperatures along the stagnation line of the 81 km CEV flow.